

See discussions, stats, and author profiles for this publication at: <https://www.researchgate.net/publication/51338121>

Wang, S., Huber, P.W., Cui, M., Czarnik, A.W. & Mei, H.Y. Binding of neomycin to the TAR element of HIV-1 RNA induces dissociation of Tat protein by an allosteric mechanism . Bioc...

ARTICLE in BIOCHEMISTRY · APRIL 1998

Impact Factor: 3.02 · DOI: 10.1021/bi972808a · Source: PubMed

CITATIONS

122

READS

21

5 AUTHORS, INCLUDING:



Shaohui Wang

GlaxoSmithKline plc.

18 PUBLICATIONS 697 CITATIONS

SEE PROFILE



Paul W. Huber

University of Notre Dame

44 PUBLICATIONS 918 CITATIONS

SEE PROFILE

Binding of Neomycin to the TAR Element of HIV-1 RNA Induces Dissociation of Tat Protein by an Allosteric Mechanism[†]

Shaohui Wang,[‡] Paul W. Huber,^{*,‡} Mei Cui,[§] Anthony W. Czarnik,[§] and Houn-Yau Mei^{*,§}

Department of Chemistry and Biochemistry, University of Notre Dame, Notre Dame, Indiana 46556, and BioOrganic Chemistry Section, Department of Chemistry, Parke-Davis Pharmaceutical Research, Division of Warner-Lambert Company, Ann Arbor, Michigan 48106

Received November 17, 1997; Revised Manuscript Received February 24, 1998

ABSTRACT: Neomycin inhibits the binding of Tat-derived peptides to the *trans*-activating region (TAR) of HIV-1 RNA. Kinetic studies reveal that neomycin acts as a noncompetitive inhibitor that can bind to the Tat–TAR complex and increase the rate constant (k_{off}) for dissociation of the peptide from the RNA. Neomycin effects a conformational change in the structure of TAR that can be detected by circular dichroism spectroscopy. The increase in ellipticity measured at 265 nm upon binding of the aminoglycoside is opposite to the decrease seen when Tat peptides bind to the RNA. Thus, the structural transition induced by neomycin is apparently incompatible with the binding of Tat and underlies the inhibitory action of the antibiotic. The binding site for neomycin on TAR was identified in ribonuclease protection experiments and is located in the stem immediately below the three-nucleotide bulge that serves as the primary identity element for Tat. Apparent protection of residues in the bulge by neomycin may represent additional contacts to the aminoglycoside, but more likely result from changes in the structure of this region when the ligand binds to the RNA. Binding assays using variants of TAR in which inosine residues were substituted for guanosine residues support the results from the ribonuclease protection experiments. Inosine substitutions in the lower stem, but not the upper stem, decrease the binding constant for neomycin by approximately 100-fold. Neither of these variants affected the binding affinity of Tat peptide. In addition, these latter experiments suggest that the aminoglycoside may be located in the minor groove of the stem. This mode of association may be a critical aspect of neomycin's ability to bind to the Tat–TAR complex and could serve as a guide for the design of other drugs that bind to specific RNA targets as noncompetitive inhibitors.

Several antibiotics exert their effects by interacting not with proteins, but rather with nucleic acids (1). Members of the aminoglycoside family of antibiotics have been shown to target a wide variety of RNA molecules, including the functionally active regions of ribosomal RNA (2–5), group I intron RNA (6), hammerhead RNA (7), human hepatitis delta virus ribozyme (8), and the RNA of human immunodeficiency virus (HIV)¹ (9, 10). Other RNA motifs that bind aminoglycosides with high affinity have been generated using *in vitro* selection techniques (11–13).

Transcription of the HIV genome is facilitated by the viral protein Tat which activates and stabilizes the synthesis of full-length HIV-1 mRNA through its binding to the *trans*-activating region designated TAR (14, 15). Recent experiments have demonstrated that some aminoglycosides can prevent the binding of Tat-derived peptides to TAR RNA (10). The TAR element, which comprises the first 59 nucleotides of the HIV-1 primary transcript, adopts a hairpin structure with a 3-nucleotide (UCU) bulge located 4 base pairs below the loop. This bulge provides the identity element for Tat which binds through the major groove at this site (16–20). The binding affinity and characteristics of Tat peptides, consisting of a highly basic domain encompassing amino acid residues 47–58, are remarkably similar to the full-length protein (21–23). Among the aminoglycoside antibiotics, neomycin (Figure 1) has the greatest inhibitory effect on Tat binding to TAR with an IC_{50} value of less than 1 μM . This inhibition is due to the direct association of the antibiotics with TAR, which can be measured by a shift in the mobility of this RNA in nondenaturing polyacrylamide gels (10). This assay was used to demonstrate a correlation between the affinities of these antibiotics for TAR and their ability to inhibit binding of a Tat peptide.

[†] Financial support was received from the University of Notre Dame and Parke-Davis Pharmaceutical Research.

^{*} To whom correspondence should be addressed. For P.W.H.: Department of Chemistry and Biochemistry, University of Notre Dame, Notre Dame, IN 46556. Phone: 219-631-6042. Fax: 219-631-6652. E-mail: Huber.1@nd.edu. For H.-Y.M.: Department of Chemistry, Parke-Davis Pharmaceutical Research, 2800 Plymouth Rd., Ann Arbor, MI 48105. Phone: 734-622-3031. Fax: 734-622-5019. E-mail: MEIH@aa.wl.com.

[‡] University of Notre Dame.

[§] Parke-Davis Pharmaceutical Research.

¹ Abbreviations: HIV-1, human immunodeficiency virus type 1; TAR, *trans*-activating region; CD, circular dichroism; NOE, nuclear Overhauser enhancement.

In the present study, we show that neomycin disrupts the Tat–TAR interaction by increasing the rate constant for dissociation of the complex. The aminoglycoside induces a structural change in the RNA, detected by circular dichroism spectroscopy, that likely underlies its effect on the stability of the complex. We have determined that the contact site for neomycin is located in the lower stem of the TAR element with the antibiotic most likely positioned in the minor groove. Disruption of the Tat–TAR complex by the antibiotic, therefore, occurs through an allosteric mechanism.

EXPERIMENTAL PROCEDURES

Materials. Neomycin sulfate (>85% neomycin B) and RNase T₁ were purchased from Sigma, and RNase V1 was from Pharmacia. Tat₄₀ and Tat₁₂ (Figure 1) were synthesized by solid-phase peptide synthesis and purified by reversed-phase HPLC. The carboxyl-terminal residue in Tat₁₂ was changed from proline to glycine to improve the synthesis of this peptide; the substitution has no effect on RNA binding. The molecular masses of purified Tat₄₀ (5663 Da) and Tat₁₂ (1616 Da) were determined by electrospray mass spectrometry (10).

Synthesis and Labeling of RNA. TAR₃₁ RNA (representing residues 18–44 of the native TAR element) and its inosine mutants were synthesized on an ABI Model 394 DNA synthesizer (Applied Biosystems) using 2'-O-silyl-protected phosphoramidites. Standard procedures were followed for deprotection of the synthetic oligonucleotides which were then purified by electrophoresis on 20% polyacrylamide gels containing 7 M urea. RNA was eluted from gel slices in 0.6 M sodium acetate (pH 6.0), 10 mM EDTA containing 0.1% SDS. The sample was then extracted 3 times with water-saturated phenol and 3 times with ether and then precipitated with ethanol. The concentration of RNA samples was determined spectrophotometrically at 260 nm using an extinction coefficient of 17.3 (mg/mL)⁻¹ cm⁻¹. RNA was labeled either at the 3' end with cytidine 3',5'-[5'-³²P]-bisphosphate, synthesized according to England et al. (24), using T4 RNA ligase (New England Biolabs), or at the 5' end with [γ -³²P]ATP using T4 polynucleotide kinase (Epicentre Technologies). All RNA samples were renatured by heating to 90 °C for 5 min followed by slow cooling to room temperature in buffer containing 10 mM Tris·HCl (pH 7.5) and 0.1 mM EDTA.

Mobility Shift Gel Assays. Binding of Tat₄₀ and neomycin to TAR₃₁ and its derivatives was measured by a shift in the mobility of the RNA in nondenaturing 20% polyacrylamide gels (75:1 acrylamide:bisacrylamide) run at room temperature at 20 V/cm (10). Binding reactions (100 μ L) were performed in buffer containing 10 mM Tris·HCl (pH 7.5), 70 mM NaCl, 0.2 mM EDTA, 0.01% NP 40, and 5% glycerol (10). After a 5 min incubation, an 8 μ L aliquot of each binding reaction was taken for electrophoresis. After drying, gels were exposed to X-ray film and the autoradiographs scanned with a laser densitometer (Molecular Dynamics). In kinetic experiments complexes were first formed between [³²P]-labeled TAR RNA and Tat₄₀ or neomycin and then the competing ligand was added in a 1/100 volume, mixed quickly, with 8 μ L aliquots taken as a function of time and loaded onto a running polyacrylamide gel.

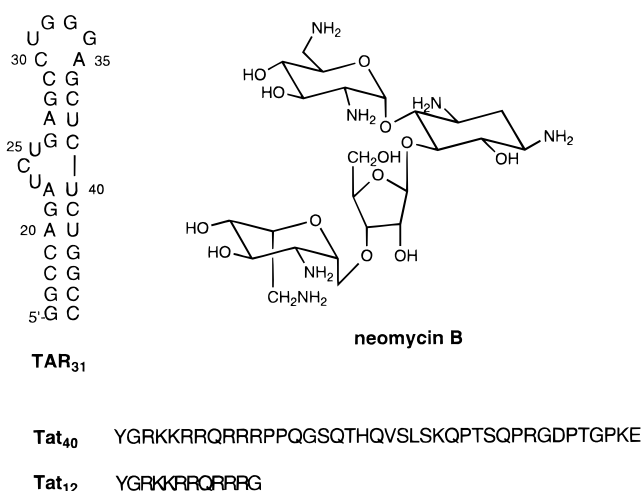


FIGURE 1: Structural diagrams of TAR₃₁ and neomycin B; the primary sequences of Tat₄₀ and Tat₁₂.

Circular Dichroism Spectroscopy. CD spectra were measured at 23 °C on a Cary 60 spectropolarimeter with modifications by Aviv. RNA was prepared as a 2 μ M solution in buffer containing 10 mM Tris·HCl (pH 7.5), 70 mM NaCl, and 0.2 mM EDTA. Each sample was scanned from 320 to 220 nm with data collection every 1 nm at a bandwidth of 1.5 nm. Each spectrum is the average of 12 scans; curves were not smoothed. A spectrum of the buffer was used to generate a base line that was subtracted from each sample spectrum. The initial sample volume of TAR RNA was 2.5 mL. Tat₁₂ or neomycin was added in 25 μ L aliquots to give the final concentration indicated; each spectrum is corrected for dilution.

RNase T1 and V1 Footprinting. RNase protection assays (10 μ L) were carried out at room temperature in 10 mM Tris·HCl (pH 7.5), 70 mM NaCl. The indicated amounts of RNA and neomycin were incubated for 5 min before the addition of 1 μ L of RNase T₁ (4 units) or V1 (4.5 \times 10⁻⁴ units). The digestion reactions were stopped after 5 min with 5 μ L of formamide loading buffer. Samples were analyzed by electrophoresis on 20% polyacrylamide sequencing gels.

RESULTS

Neomycin Promotes Dissociation of the Tat–TAR Complex. Several of the aminoglycoside antibiotics can block binding of Tat peptide to TAR₃₁ RNA (10). This inhibition is due to the direct binding of the antibiotics to the nucleic acid which can be detected by electrophoresis on nondenaturing polyacrylamide gels (mobility shift assays). The ability to inhibit binding of Tat was shown to correlate well with the affinity of the particular aminoglycoside for TAR.

The major identity elements for Tat are located in the three-nucleotide bulge and the upper stem region of the TAR hairpin (Figure 1) (16, 18–20, 25, 26). However, competition assays with variants of TAR that either lack the bulged nucleotides or have replaced them with a poly(ethylene glycol) linker show little reduction in affinity for neomycin (10). Mutations in the loop region also have little effect on the binding of the antibiotic. These results indicate that, despite their mutually exclusive binding, the aminoglycosides and Tat use distinct recognition elements on TAR RNA.

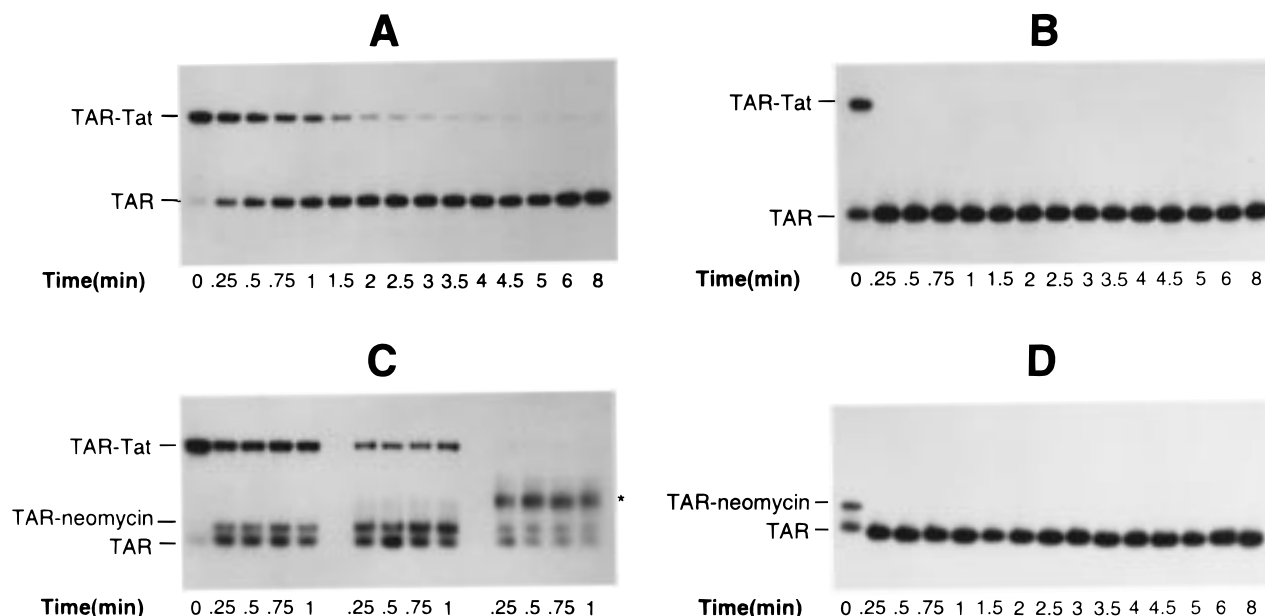


FIGURE 2: Dissociation kinetics of the Tat₄₀-TAR₃₁ complex. Complexes between ³²P-labeled TAR (~0.1 nM) and 3 nM Tat₄₀ (panels A–C) or 10 μM neomycin (panel D) were formed and then challenged with the indicated ligand. Aliquots of the reaction mixture were taken as a function of time and loaded onto a running 20% polyacrylamide gel. (A) Tat–TAR complex challenged with 20 nM unlabeled TAR₃₁. (B) Tat–TAR complex challenged with 20 nM unlabeled TAR₃₁ and 10 μM neomycin. (C) Tat–TAR complex challenged with 10 μM neomycin (first 5 lanes), 100 μM neomycin (middle 4 lanes), and 1 mM neomycin (last 4 lanes). The asterisk denotes bands representing a higher-order complex between TAR₃₁ and neomycin that likely correspond to the TAR/neomycin₂ species detected in ESI-MS experiments (44). (D) Neomycin–TAR complex challenged with 20 nM unlabeled TAR₃₁.

The rate constant for the dissociation of the Tat–TAR complex (k_{off}) was measured by forming a complex between ³²P-labeled TAR RNA and Tat₄₀ peptide and then challenging the complex with an excess of unlabeled TAR (23). Aliquots of the reaction mixture were taken as a function of time and loaded onto a running polyacrylamide gel (Figure 2A). An autoradiograph of the gel was scanned with a laser densitometer in order to quantitate the amount of radiolabeled complex at each time point. The disappearance of the Tat₄₀–TAR₃₁ complex follows a first-order rate equation with a half-life of 41 s. Somewhat longer half-lives have been measured for other Tat-derived peptides in slightly different binding conditions (23). When 10 μM neomycin is included with unlabeled TAR, the dissociation of the ³²P-labeled complex is now complete before the first sample can be taken for analysis (Figure 2B). This result establishes that neomycin does not simply compete with the peptide for binding to the RNA, but rather the antibiotic binds and facilitates dissociation of Tat from the resulting ternary complex.

The effect of neomycin on the Tat–TAR complex in the absence of excess TAR RNA was tested in the experiment shown in Figure 2C. The complex was challenged with one of three concentrations of neomycin: 10 μM (lanes 2–5, left panel), 100 μM (lanes 6–9, center panel), and 1 mM (lanes 10–13, right panel). In each case, the amount of Tat–TAR complex remaining is inversely proportional to the amount of neomycin added. Moreover, the effect is immediate; binding of the antibiotic and disruption of the RNP complex are completed before the first time point of the assay. Free TAR RNA is observed in Figure 2C, despite the presence of saturating concentrations of Tat and neomycin. We believe this uncomplexed RNA arises from a ternary complex comprised of Tat, TAR, and neomycin which we presume is unstable in the conditions of electrophoresis. The presence of this ternary complex has been

detected by electrospray ionization mass spectrometry (ESI-MS); those experiments also demonstrate that neomycin binds only to TAR with no apparent affinity for Tat (27). We have attempted to determine, in the absence of Tat, the kinetic parameters of neomycin binding to TAR. However, the complex is in rapid equilibrium, and neither the rate constant for formation nor the rate constant for dissociation (Figure 2D) can be measured using the mobility shift assay.

Together, the results of these kinetic experiments establish that neomycin is not a competitive inhibitor with respect to Tat₄₀, which is consistent with the ability of the aminoglycosides to bind to variants of TAR that do not bind the peptide (10). The rapid binding of neomycin to form a ternary complex, instead, increases the rate of dissociation of Tat from TAR.

Neomycin Induces a Change in the Structure of TAR. NMR studies have revealed that the binding of Tat peptide (20) or simply argininamide (17) triggers a substantial transformation in the structure of TAR RNA involving nucleotides within the bulge and upper-stem region. This conformational change can be monitored by circular dichroism (CD) spectroscopy (23, 28, 29). We considered the possibility that the displacement of Tat by neomycin could be the consequence of a change in the structure of the RNA either back to the conformation of the free nucleic acid or to one incompatible with the binding of the peptide. Therefore, we examined the effect of neomycin on the CD spectrum of TAR₃₁. The binding of a 12 amino acid Tat peptide causes a modest decrease in the peak of positive rotation centered at 265 nm (Figure 3A) comparable to spectra reported by others (23, 28, 29). Neomycin also alters the CD spectrum of TAR₃₁; however, unlike Tat, the aminoglycoside increases the ellipticity of the positive peak with a concomitant shift to longer wavelengths. This result demonstrates not only that neomycin induces a change in

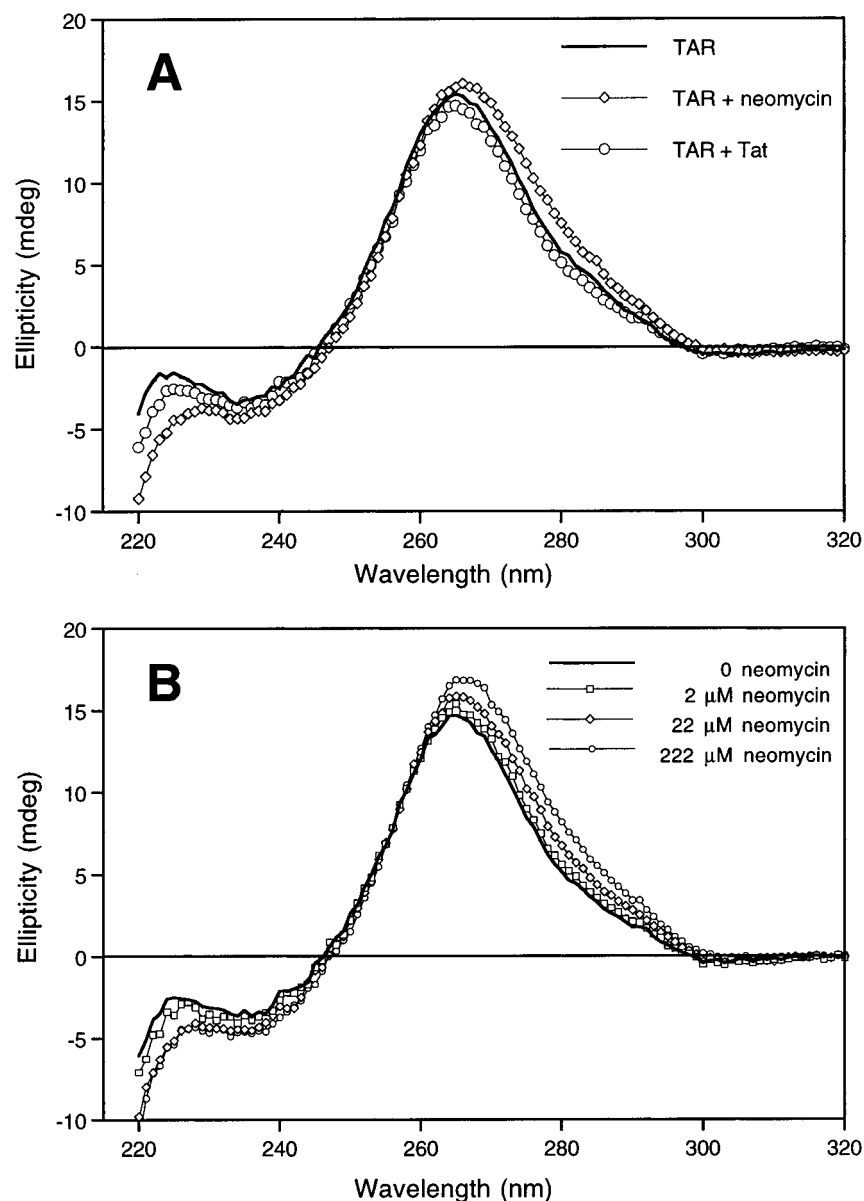


FIGURE 3: Conformational changes in TAR₃₁ measured by CD spectroscopy. (A) Spectra of 2 μ M TAR₃₁ alone or in the presence of either 2 μ M Tat₁₂ peptide or 22 μ M neomycin. (B) A sample containing 2 μ M TAR₃₁ and 2 μ M Tat₁₂ was titrated with increasing concentrations of neomycin. The spectra displaying increasing ellipticity at 265 nm correspond to samples containing 0, 2, 22, and 222 μ M neomycin, respectively.

the RNA upon binding but also that this structure is distinct from that seen in the Tat–TAR complex.

We titrated the Tat₁₂–TAR complex with increasing concentrations of neomycin in order to demonstrate directly the structural change in TAR₃₁ that accompanies displacement of the peptide by the antibiotic (Figure 3B). The increase in ellipticity at 265 nm is proportional to the amount of neomycin added to the sample of Tat₁₂–TAR₃₁ complex. The results from this solution experiment are in accord with those from the mobility shift assays (Figure 2C) that demonstrated the ability of neomycin to disrupt the Tat–TAR complex. The small change in ellipticity limited the number of steps in the titration; nonetheless, the spectral transition occurs over a concentration range of neomycin consistent with the dissociation constant (~ 1 μ M) measured in mobility shift assays.

Identification of the Binding Site for Neomycin on TAR₃₁. Binding assays testing several variants of TAR indicate that

the loop and bulge regions of the hairpin are not the primary identity elements for neomycin (10). The results of the kinetic experiments presented here (Figure 2) and the ESI-MS experiments (27) indicate that neomycin is a noncompetitive inhibitor with respect to Tat that can form a ternary complex with Tat–TAR. These data support the conclusion that the three-nucleotide bulge is not the primary contact site for neomycin. We undertook chemical protection experiments in order to locate the binding site for neomycin on TAR₃₁. In our initial experiments using chemical probes such as dimethyl sulfate and diethyl pyrocarbonate, we could not detect any protection of TAR₃₁ by neomycin. However, the majority of chemical reagents used to analyze RNA structure either target positions involved in base pair hydrogen bonding or are poorly accessible to positions in helical structures due to stacking interactions (30). Consequently, it is difficult to identify binding sites in double-stranded regions. In addition, sites that react with these

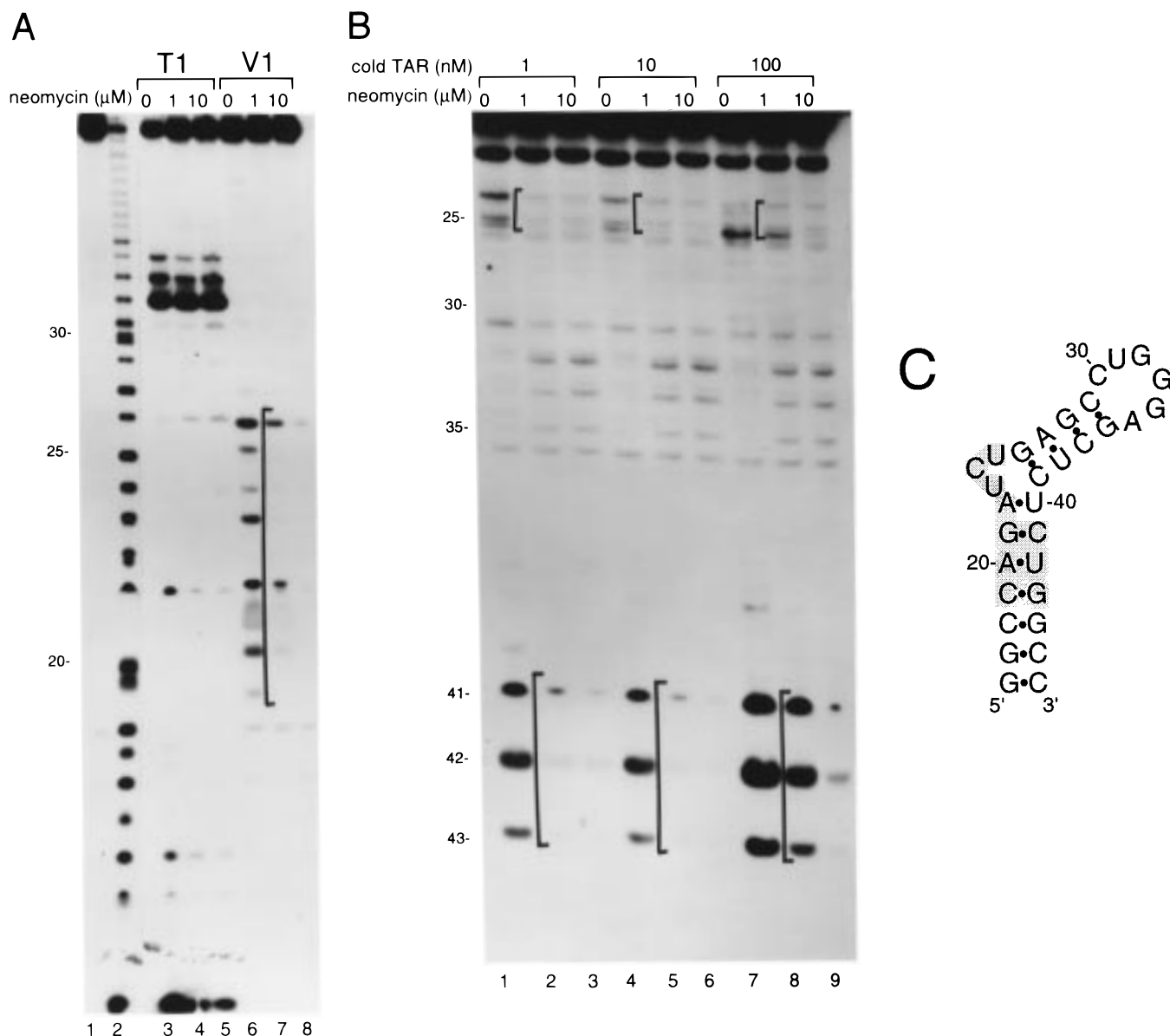


FIGURE 4: RNase protection analysis of the neomycin-TAR₃₁ complex. (A) TAR RNA labeled with ^{32}P at the 5'-terminus was incubated without (lanes 3 and 6) or in the presence of 1 μM (lanes 4 and 7) or 10 μM (lanes 5 and 8) neomycin. Samples were digested with either RNase T1 (lanes 3–5) or RNase V1 (lanes 6–8) for 5 min at room temperature and the products analyzed by electrophoresis followed by autoradiography. Lane 1 is untreated control RNA, and lane 2 is a partial alkaline hydrolysis. (B) TAR RNA labeled with ^{32}P at the 3'-terminus (~ 0.1 nM) was used in competition binding assays. The total concentration of unlabeled RNA was kept constant at 100 nM as the ratio of tRNA (nonspecific competitor) to TAR₃₁ (specific competitor) was varied from 99 to 0. Protection was determined at 0 (lanes 1, 4, and 7), 1 μM (lanes 2, 5, and 8), and 10 μM neomycin (lanes 3, 6, and 9). Brackets enclose regions of the RNA protected from hydrolysis by neomycin. (C) The regions of TAR₃₁ protected from V1 digestion by neomycin are indicated on the secondary structure of the RNA by stippling.

chemical probes are almost exclusively located in the major groove.

Because of these limitations, we turned to protection experiments using ribonucleases T1 and V1; the former is specific for single-stranded guanines while the latter is a structure-specific nuclease that cleaves double-stranded regions. As expected, the primary sites of hydrolysis by T1 are the three guanines located at loop positions 32–34 (Figure 4A, lane 3); neomycin has no effect on cleavage at these sites (lanes 4 and 5). Weak cleavage at residue G₂₁ in the lower stem, however, is lost in the presence of neomycin. Hydrolysis by V1 occurs in the lower stem of TAR₃₁ and includes sites within the three-nucleotide bulge (Figure 4A, lane 6, and Figure 4B, lane 1). It should be noted that the

products of V1 cleavage, unlike those of T1 and alkaline hydrolyses, contain a 5'-phosphate which alters their electrophoretic migration relative to the other two. Neomycin protects several sites in the lower stem and the three-nucleotide bulge from digestion with V1. The region of protection extends from nucleotide 19 through nucleotide 26 on the 5' side (Figure 4A, lanes 7 and 8) and from nucleotide 41 through nucleotide 43 on the 3' side of the hairpin (Figure 4B, lanes 2 and 3). There is no appreciable cleavage by V1 in the upper stem region of TAR between the bulge and the loop, so this segment remains untested in these experiments. Residue G₂₆ is not as well protected by neomycin relative to the other positions cut by ribonuclease V1 in the lower stem (Figure 4A, lanes 6 and 7); conversely, this residue

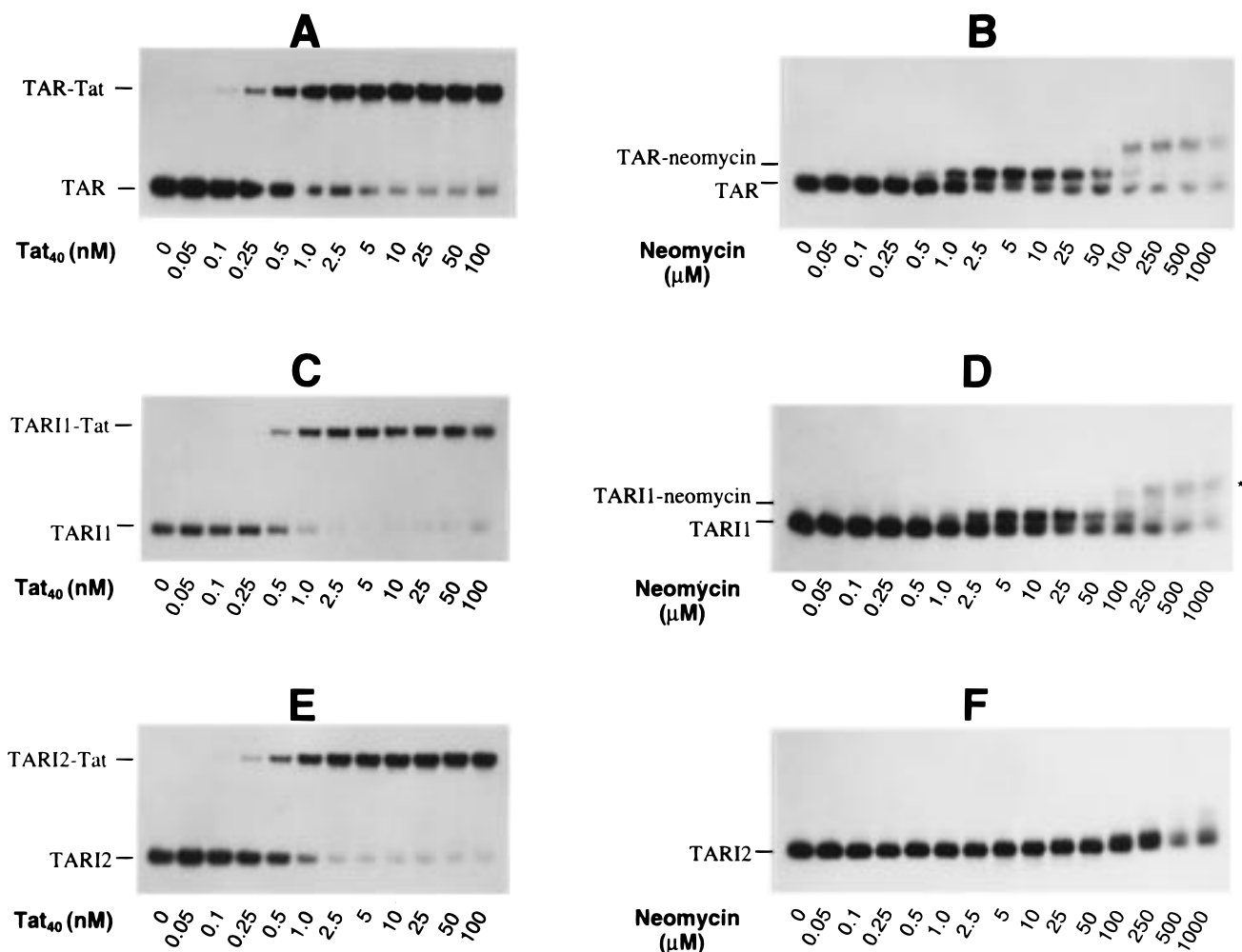


FIGURE 5: Mobility shift assays for binding of Tat₄₀ and neomycin to inosine mutants of TAR₃₁. In each assay ~ 0.1 nM 32 P-labeled RNA was incubated with the designated concentration of Tat₄₀ (A, C, and E) or neomycin (B, D, and F). Binding affinities were measured using wild-type TAR RNA (A and B), TARI1 in which the guanosines of the upper stem were replaced by inosine (C and D), or TARI2 in which the guanosines of the lower stem were replaced by inosine (E and F). Asterisks denote bands that correspond to higher order complexes formed between TAR and neomycin (44).

becomes weakly susceptible to cleavage by T1 in the presence of neomycin (Figure 4A, lane 5). These observations suggest that the border of the neomycin binding site is situated in the vicinity of G₂₆ and most likely does not include the upper stem region.

Hydrolysis by V1 at the three-nucleotide bulge was unexpected; however, this ribonuclease can cleave unpaired single nucleotides that are stacked upon double helices (31–33). Recent cross-linking (34) and NMR (35) studies with TAR RNA indicate that nucleotides U₂₃ and C₂₄ of the bulge are stacked within the helical stem which potentially explains their susceptibility to V1. It is important to note, then, that the loss of cleavage at the bulged nucleotides in the TAR–neomycin complex may not necessarily be due to direct protection by the aminoglycoside, but rather could result from an unstacking of these nucleotides upon binding neomycin. This type of structural transition would also account for the weak hydrolysis by T1 at G₂₆ that occurs only in the presence of the antibiotic. The region of apparent protection from V1 hydrolysis by neomycin is shown on the secondary structure of TAR₃₁ in Figure 4C.

Since most of the sites of V1 hydrolysis in the lower stem of TAR₃₁ are diminished by the addition of neomycin, we performed a competition experiment to establish that the

observed reduction in cleavage was due to specific binding of the antibiotic and not to some effect on the activity of the ribonuclease. Protection by neomycin from V1 cleavage was tested at increasing concentrations of unlabeled TAR₃₁ RNA (Figure 4B). The observed amount of cleavage of radio-labeled RNA by the ribonuclease will be sensitive to the total amount of RNA present in the reaction mixture; therefore, the concentration of RNA was kept constant at 100 nM by varying the ratio of unlabeled TAR RNA to unlabeled tRNA. In the presence of 1 and 10 nM unlabeled TAR RNA, there is no loss of the protection pattern in the lower stem (Figure 4B, lanes 2, 3, 5, and 6); however, in the presence of 100 nM unlabeled TAR, protection at 1 μ M neomycin is essentially abolished and protection at 10 μ M antibiotic is not complete (Figure 4B, lanes 8 and 9). The competition by cold TAR as well as the absence of any effect by the corresponding amount of tRNA (Figure 4B, lanes 1–3) establishes that the observed protection pattern is due to binding of the aminoglycoside to a specific site on the RNA.

Effect of Inosine Substitutions on the Binding of Neomycin to TAR₃₁. To confirm the results from the protection experiments, we tested binding of neomycin to variants of TAR₃₁ in which the guanosines in the upper (TARI1) or

lower (TARI2) stems were replaced by inosine. Compared with guanosine, inosine lacks the base-pairing, N2 exocyclic amino group that is positioned in the minor groove of double-helical regions. The reduced number of base pair hydrogen bonds will lower the thermal stability of these variants (36, 37). Therefore, as a control to ensure that the inosine mutants assume the same secondary structure as TAR₃₁, we compared binding of Tat₄₀ to wild-type RNA with binding to the two inosine variants (Figure 5). The binding affinities of Tat for TARI1 (Figure 5C) and TARI2 (Figure 5E) are identical to that for the wild-type RNA (Figure 5A), indicating that there is no substantial distortion of secondary structure in the inosine variants. However, it must be kept in mind that a double-helical region with I·C base pairs may still be conformationally different from one with G·C base pairs both for steric and for dynamic reasons (38).

The binding affinity of neomycin for TARI1 (Figure 5D) is quite similar to that for the unsubstituted RNA (Figure 5B); however, the antibiotic has a greatly diminished affinity for TARI2 (Figure 5F). Some binding to TARI2 becomes apparent beginning at 100 μ M aminoglycoside, indicating that the affinity of neomycin for this variant RNA is at least 100-fold less than for the wild-type RNA. These results, likewise, identify the lower stem of TAR as the binding site for neomycin, corroborating the protection experiments. Notwithstanding the caveat concerning differences in stabilities among the inosine variants and the unsubstituted RNA, these results also suggest that neomycin may bind to TAR through the minor groove. This mode of binding would be consistent with our experiments that failed to detect protection from chemical probes that target positions in the major groove. We have attempted to identify critical contact sites for neomycin by making individual replacements of inosine for guanosine at positions in the lower stem; however, none of these single substitutions produced an appreciable reduction in binding of the aminoglycoside. This indicates that the reduced affinity of neomycin for TARI2 does not result from the removal of a critical contact to one of the N2 amino groups, but is more likely due to an alteration in the conformation of the stem.

DISCUSSION

We reported earlier that aminoglycoside antibiotics can prevent the binding of Tat peptides to TAR due to a direct association of the antibiotics with this RNA (10). The current experiments extend that work by showing that neomycin induces a change in the structure of TAR RNA that is apparently incompatible with the binding of Tat. The binding site for neomycin is located in the lower stem of TAR which allows for the transient formation of a Tat–TAR–neomycin ternary complex. Thus, the antibiotic behaves as a noncompetitive inhibitor of Tat which is apparent in our kinetic experiments that demonstrate neomycin increases the rate constant, k_{off} , for dissociation of the peptide–RNA complex. A minimal scheme highlighting the inhibitory mechanism of neomycin is presented in Figure 6.

There are several key elements of this model. Three distinct conformations of TAR are apparent in our CD experiments. The structure of TAR has been studied by NMR spectroscopy (17, 35). Both imino proton resonances

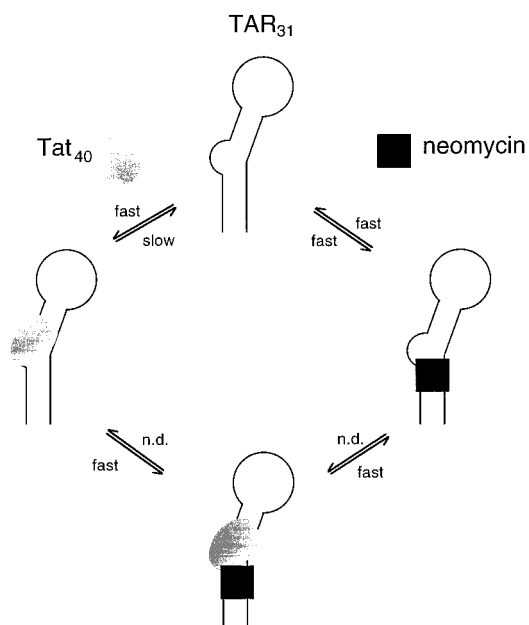


FIGURE 6: Kinetic model for the interactions among TAR, Tat, and neomycin. No attempt has been made to represent the different conformations of TAR RNA. Steps for which there is no kinetic information are marked n.d.

and NOE interactions indicate that the two stems surrounding the bulge have a standard A-form geometry (35). However, the high solvent exchange seen for the imino proton of U₄₀ as well as the absence of NOE cross-peaks between A₂₂ and U₄₀ suggest that this base pair at the junction between the lower stem and the internal bulge is unstable or has an atypical geometry. In addition, three purine residues, A₂₀, G₂₁, and A₂₂, in the lower stem are susceptible to modification by diethyl pyrocarbonate, indicating that the major groove is somewhat wider than that of a canonical A-form helix (16). Consequently, to a corresponding degree, the minor groove will be deeper and more narrow. These subtle perturbations in the structure of the lower stem may underlie the high-affinity binding of neomycin to this region of TAR.

The binding of Tat engenders substantial changes in the structure of TAR that involve residues in the bulge and immediately flanking residues of the upper stem (17, 20, 35). Although there is no conclusive evidence that Tat induces structural changes in the lower stem, chemical modification of phosphates P22, P23, and P40 does interfere with binding. Moreover, an NOE between the H2 proton of A₂₂ and the H3 imino proton of U₄₀, absent in the spectrum of free TAR, is present in the spectrum of the peptide-bound RNA, suggesting that this base pair is stabilized in the complex (20).

The substantial differences in the structure of free and Tat-bound TAR are reflected in changes in the CD spectra of the RNA (23, 28, 29). It has been noted by Long and Crothers (23) that the decrease in ellipticity at 260 nm upon binding Tat peptides is consistent with the unstacking of bases in the bulge region seen in the structures derived by NMR and molecular dynamics. The CD spectrum of the neomycin–TAR complex exhibits a distinct increase in ellipticity at 260 nm, indicating an increase in base stacking in the RNA (39). Thus, it is noteworthy that new sites of moderate cleavage by ribonuclease V1 are apparent between

residues 31 and 35 when neomycin binds to TAR (Figure 4B). These positions are located in the apical loop of TAR which does not appear to be well structured in the free RNA, but which may adopt a more ordered structure upon binding of the aminoglycoside. The important observation is that the two ligands each alter TAR RNA to generate two distinct structures. This is the apparent basis for the inhibitory effect of the aminoglycosides on the binding of Tat.

The footprint of neomycin on TAR using ribonuclease V1 can only be considered an approximation of the antibiotic's contact site on the RNA, since the apparent protection pattern is a function of the binding and cleavage characteristics of the nuclease. The enhanced dissociation rate of the Tat-TAR complex in the presence of neomycin is most reasonably explained by the transient formation of a ternary complex (Figure 6) which indicates that the primary contacts of the antibiotic are in the lower stem region of TAR. The protection from V1 hydrolysis extending up into the bulge region may reflect additional contacts that could be established after the displacement of Tat. Alternatively, the apparent protection may simply be due to conformational changes in the bulge region resulting in its resistance to cleavage by the ribonuclease. Our present experiments cannot differentiate between these two cases. We can conclude, however, that essential contacts made by Tat to nucleotides in the bulge are not possible in the neomycin-induced conformation of TAR.

The binding assays with inosine mutants of TAR provide additional evidence that neomycin binds to the lower stem of TAR. Equally important, however, these experiments suggest that the aminoglycoside is positioned in the minor groove of the helix. The binding sites for aminoglycosides are invariably locations where the major groove of the RNA is opened and accessible due to mismatched (non-Watson-Crick) base pairs, bulged nucleotides, or a junction between stem and loop structures (13, 40–42). TAR possibly provides the first exception to this convention. Deletion of the three-nucleotide bulge has little effect on the affinity of neomycin for TAR (10), indicating that the antibiotic does not require a stem structure that is considerably perturbed from a canonical A-form helix. In this conformation, the major groove will not be accessible to the aminoglycoside; however, the broad and shallow minor groove can accommodate the ligand. Moreover, this mode of binding may explain the ability of TAR, Tat, and neomycin to form a detectable ternary complex (27), since the two ligands would be positioned in opposite grooves of the RNA. A significant remaining question is what changes in the structure of TAR stabilize its interaction with the aminoglycoside, since this transition disrupts the binding of Tat.

The manner in which neomycin inhibits the binding of Tat to TAR has important implications for the design of drugs that target RNA-protein complexes. Small molecules usually inhibit the function of their target RNA by competing directly for the binding sites of other biomolecules. For example, a tetrahydropyrimidine derivative modeled to fit the bulge region of TAR blocks association with Tat (43). Neomycin, however, represents the first example of a small molecule inhibitor that displaces Tat by an allosteric mechanism. Noncompetitive inhibitors that act in this way are particularly valuable because they can efficiently disrupt complexes irrespective of their half-lives, since the ligand

can associate with both free and protein-bound RNA. We believe that delineating the mechanism of action of neomycin will expedite the design of new therapeutics that target the Tat-TAR complex. This strategy should be generally applicable to similar gene regulatory complexes containing an RNA component.

ACKNOWLEDGMENT

We are grateful to Professor K. Nakanishi (Columbia University) for helpful discussions about CD spectroscopy.

REFERENCES

1. Cundliffe, E. (1981) in *The Molecular Basis of Antibiotic Action* (Gale, E. F., Cundliffe, E., Reynolds, P. E., Richmond, M. H., and Waring, M. H., Eds.) pp 402–547, Wiley, New York.
2. Moazed, D., and Noller, H. F. (1987) *Nature* 327, 389–394.
3. Egebjerg, J., Douthwaite, S., and Garrett, R. A. (1989) *EMBO J.* 8, 607–611.
4. Ryan, P. C., Lu, M., and Draper, D. E. (1991) *J. Mol. Biol.* 221, 1257–1268.
5. Purohit, P., and Stern, S. (1994) *Nature* 370, 659–662.
6. von Ahsen, U., and Noller, H. F. (1993) *Science* 260, 1500–1503.
7. Stage, T. K., Hertel, K. J., and Uhlenbeck, O. C. (1995) *RNA* 1, 95–101.
8. Rogers, J., Chang, A. H., von Ahsen, U., Schroeder, R., and Davies, J. (1996) *J. Mol. Biol.* 259, 916–925.
9. Zapp, M. L., Stern, S., and Green, M. R. (1993) *Cell* 74, 969–978.
10. Mei, H.-Y., Galan, A. A., Halim, N. S., Mack, D. P., Moreland, D. W., Sanders, K. B., Truong, H. N., and Czarnik, A. W. (1995) *Bioorg. Med. Chem. Lett.* 5, 2755–2759.
11. Lato, S. M., Boles, A. R., and Ellington, A. D. (1995) *Chem. Biol.* 2, 291–303.
12. Wallis, M. G., von Ahsen, U., Schroeder, R., and Famulok, M. (1995) *Chem. Biol.* 2, 543–552.
13. Wang, Y., and Rando, R. R. (1995) *Chem. Biol.* 2, 281–290.
14. Gait, M. J., and Karn, J. (1993) *Trends Biochem. Sci.* 18, 255–259.
15. Jones, K. A., and Peterlin, B. M. (1994) *Annu. Rev. Biochem.* 63, 717–743.
16. Weeks, K. M., and Crothers, D. M. (1991) *Cell* 66, 577–588.
17. Puglisi, J. D., Tan, R., Calnan, B. J., Frankel, A. D., and Williamson, J. R. (1992) *Science* 257, 76–80.
18. Tao, J., and Frankel, A. D. (1992) *Proc. Natl. Acad. Sci. U.S.A.* 89, 2723–2726.
19. Dellling, U., Reid, L. S., Barnett, R. W., Ma, M. Y.-X., Climie, S., Sumner-Smith, M., and Sonenberg, N. (1992) *J. Virol.* 66, 3018–3025.
20. Aboul-ela, F., Karn, J., and Varani, G. (1995) *J. Mol. Biol.* 253, 313–332.
21. Weeks, K. M., Ampe, C., Schultz, S. C., Steitz, T. A., and Crothers, D. M. (1990) *Science* 249, 1281–1285.
22. Weeks, K. M., and Crothers, D. M. (1992) *Biochemistry* 31, 10281–10287.
23. Long, K. S., and Crothers, D. M. (1995) *Biochemistry* 34, 8885–8895.
24. England, T. E., Bruce, A. G., and Uhlenbeck, O. C. (1980) *Methods Enzymol.* 65, 65–74.
25. Cordingley, M. G., LaFemina, R. L., Callahan, P. L., Condra, J. H., Sardana, V. V., Graham, D. J., Nguyen, T. M., LeGrow, K., Gotlib, L., Schlabach, A. J., and Colonna, R. J. (1990) *Proc. Natl. Acad. Sci. U.S.A.* 87, 8985–8989.
26. Calnan, B. J., Tidor, B., Biancalana, S., Hudson, D., and Frankel, A. D. (1991) *Science* 252, 1167–1171.
27. Sannes, K. A., Loo, J. A., Hu, P., Mei, H.-Y., and Mack, D. (1996) *Proceedings of the 44th ASMS Conference on Mass Spectrometry and Allied Topics*, p 1405.

28. Calnan, B. J., Hudson, D., and Frankel, A. D. (1990) *Genes Dev.* 5, 201–210.
29. Loret, E. P., Georgel, P., Johnson, W. C., Jr., and Ho, P. S. (1992) *Proc. Natl. Acad. Sci. U.S.A.* 89, 9734–9738.
30. Ehresmann, C., Baudin, F., Mougél, M., Romby, P., Ebel, J. P., and Ehresmann, B. (1987) *Nucleic Acids Res.* 15, 9109–9128.
31. Lockard, R. E., and Kumar, A. (1981) *Nucleic Acids Res.* 9, 5125–5140.
32. Auron, P. E., Weber, L. D., and Rich, A. (1982) *Biochemistry* 21, 4700–4706.
33. Lowman, H. B., and Draper, D. E. (1986) *J. Biol. Chem.* 261, 5396–5403.
34. Wang, Z., and Rana, T. M. (1996) *Biochemistry* 35, 6491–6499.
35. Aboul-ela, F., Karn, J., and Varani, G. (1996) *Nucleic Acids Res.* 24, 3974–3981.
36. Turner, D. H., Sugimoto, N., Kierzek, R., and Dreiker, S. M. (1987) *J. Am. Chem. Soc.* 109, 3783–3785.
37. Strobel, S. A., Cech, T. R., Usman, N., and Beigelman, L. (1994) *Biochemistry* 33, 13824–13835.
38. Mirau, P. A., and Kearns, D. R. (1984) *J. Mol. Biol.* 177, 207–227.
39. Riazance, J. H., Baase, W. A., Johnson, W. C., Jr., Hall, K., Cruz, P., and Tinoco, I., Jr. (1985) *Nucleic Acids Res.* 13, 4983–4989.
40. Fourmy, D., Recht, M. I., Blanchard, S. C., and Puglisi, J. D. (1996) *Science* 274, 1367–1371.
41. Jiang, L., Suri, A. K., Fiala, R., and Patel D. J. (1997) *Chem. Biol.* 4, 35–50.
42. Werstuck, G., Zapp, M. L., and Green, M. R. (1996) *Chem. Biol.* 3, 129–137.
43. Lapidot, A., Ben-Asher, E., and Eisenstein, M. (1995) *FEBS Lett.* 367, 33–38.
44. Sannes-Lowery, K. A., Mei, H.-Y., Mack, D. P., and Loo, J. A. (1997) *Proceedings of the 45th ASMS Conference on Mass Spectrometry and Allied Topics*, p 1390.

BI972808A